

Rechargeable cathodes based on $\text{Li}_2\text{Cr}_x\text{Mn}_{2-x}\text{O}_4$

I.J. Davidson *, R.S. McMillan, J.J. Murray

Institute for Environmental Research and Technology, National Research Council Canada, Ottawa, Ont., K1A 0R6, Canada

Abstract

Phases in the solid-state solution series $\text{Li}_2\text{Cr}_x\text{Mn}_{2-x}\text{O}_4$ were prepared as single-phase compounds over the range $0 < x < 2$. The unit cell volume decreases smoothly with increasing chromium content as Cr^{3+} , with a smaller ionic radius, is substituted for Mn^{3+} . The X-ray powder diffraction patterns of phases in the range $1.5 \leq x < 2$ are similar to that of LiCrO_2 , while the diffraction patterns of $\text{Li}_2\text{Cr}_x\text{Mn}_{2-x}\text{O}_4$ phases over the range $0 < x \leq 1.25$ resemble that of $\lambda\text{-Li}_2\text{Mn}_2\text{O}_4$. Selected phases of $\text{Li}_2\text{Cr}_x\text{Mn}_{2-x}\text{O}_4$ were formed into cathodes and evaluated in lithium-ion cells with petroleum coke-based anodes.

Keywords: Rechargeable cathodes; Lithium; Chromium; Manganese

1. Introduction

LiCrO_2 has a hexagonal structure like that of LiCoO_2 and LiNiO_2 in which the transition metal and lithium atoms are arranged in alternating layers perpendicular to the *c*-axis. LiMnO_2 has a unique orthorhombic structure which was identified by Hoppe et al. [1]. Since LiMnO_2 and LiCrO_2 have quite different structures, it was somewhat surprising to find that they are completely miscible. Solid-state solution phases of $\text{Li}_2\text{Cr}_x\text{Mn}_{2-x}\text{O}_4$ were obtained over the full range of composition, $0 < x < 2$, but a major structural change occurs near $x = 1.25$. The X-ray powder diffraction patterns of phases in the range $1.5 \leq x < 2$ are similar to that of LiCrO_2 , with the exception that the reflections are shifted to slightly lower diffraction angles, corresponding to larger unit cell size. The magnitude of the shift increases as x decreases from 2 to 1.5, and is accompanied by a change in color from olive green for LiCrO_2 to dark brown for $\text{Li}_2\text{Cr}_{1.5}\text{Mn}_{0.5}\text{O}_4$.

The X-ray powder diffraction patterns of $\text{Li}_2\text{Cr}_x\text{Mn}_{2-x}\text{O}_4$ phases for compositions with $0 < x \leq 1.25$ resemble the diffraction pattern of $\lambda\text{-Li}_2\text{Mn}_2\text{O}_4$, which has a tetragonal unit cell with a spinel-related atacamite-type structure. Both LiMn_2O_4 and $\lambda\text{-Li}_2\text{Mn}_2\text{O}_4$ have been used as cathodes in lithium-ion cells. $\lambda\text{-Li}_2\text{Mn}_2\text{O}_4$ has twice the nominal capacity of LiMn_2O_4 but it is reported to be hygroscopic and metastable [2]. $\lambda\text{-Li}_2\text{Mn}_2\text{O}_4$ converts to the orthorhombic form,

LiMnO_2 , at about 500 °C. It is prepared by electrochemically, or chemically, intercalating lithium into the LiMn_2O_4 spinel structure. Doping $\text{Li}_2\text{Mn}_2\text{O}_4$ with chromium apparently stabilize the lambda structure. $\text{Li}_2\text{Cr}_x\text{Mn}_{2-x}\text{O}_4$, with $0.1 \leq x \leq 1.25$, can be prepared, directly, at 1000 °C by solid-state reaction.

The use of related phases such as $\text{LiMn}_{2-x}\text{Cr}_x\text{O}_{4.35}$ with x from about 0.2 to about 0.4, and $\text{LiCr}_x\text{Mn}_{2-x}\text{O}_4$ where $0 < x < 1$ as cathodes in secondary lithium batteries which have a metallic lithium anode has been described previously [3,4]. In the latter case, electrochemical insertion of one mole equivalent of lithium into $\text{LiCr}_x\text{Mn}_{2-x}\text{O}_4$ would result in a phase of the same stoichiometry, although not necessarily the same structure as one of those described here. However, the authors only managed to electrochemically insert about 0.4 mole equivalents of lithium.

2. Experimental

Single-phase compositions of $\text{Li}_2\text{Cr}_x\text{Mn}_{2-x}\text{O}_4$ were prepared by two methods. In the first, Li_2CO_3 (Aldrich 99.997%), Cr_2O_3 (Fisher Certified Reagent) and $\beta\text{-MnO}_2$ (Fisher Certified Reagent), were intimately mixed, pelletized and then reacted in a flow of argon gas. The reagents were initially calcined at 600 °C for 3 h and then held at 1000 °C for three days. The second method of preparing $\text{Li}_2\text{Cr}_x\text{Mn}_{2-x}\text{O}_4$ phases was similar to the first except that stoichiometric combinations of LiCrO_2 and orthorhombic LiMnO_2 were

* Corresponding author.

used as the starting materials and the pelletized samples were reacted at 1000 °C in argon. The orthorhombic LiMnO_2 was prepared from Li_2CO_3 and $\beta\text{-MnO}_2$ calcined at 600 °C, and then reacted at 800 °C, in argon. The LiCrO_2 was made by reacting Li_2CO_3 and Cr_2O_3 , in air, at 700 °C. The progress of the reactions was followed by X-ray powder diffraction. In most cases, two or three repeated grindings and firings were required to obtain a homogeneous product.

A range of compositions of $\text{Li}_2\text{Cr}_x\text{Mn}_{2-x}\text{O}_4$ were evaluated in lithium-ion cells. These cells were assembled in a 2325 coin cell format with anodes containing petroleum coke combined with 7.5 wt.% Super S carbon black (Chemetals Inc.) and 2 wt.% ethylene/propylene/diene monomer (EPDM) binder (Polysar) and cathodes of $\text{Li}_2\text{Cr}_x\text{Mn}_{2-x}\text{O}_4$ with 10 wt.% Super S carbon black and 2 wt.% EPDM. The cells employed a polypropylene felt separator (Web Dynamics) and contained an electrolyte solution of 1 M $(\text{CF}_3\text{SO}_2)_2\text{N}^-\text{Li}^+$ (3M company) in a 50/50 mixture by volume of propylene carbonate and dimethoxyethane.

3. Results and discussion

The diffraction patterns of $\text{Li}_2\text{Cr}_x\text{Mn}_{2-x}\text{O}_4$ were indexed to hexagonal cells for compositions with $1.5 \leq x \leq 1.9$, and to tetragonal unit cells for composition in the range $1.25 \leq x \leq 0.1$. The change in lattice parameters with increasing chromium substitution is illustrated in Fig. 1. $\lambda\text{-Li}_2\text{Mn}_2\text{O}_4$ has a tetragonal structure of dimensions $a = 5.652 \text{ \AA}$ and $c = 9.329 \text{ \AA}$ belonging to the space group $I4_1/amd$ [5]. The X-ray powder pattern of $\text{Li}_2\text{CrMnO}_4$ can be approximately indexed to a tetragonal unit cell with $a = 5.74 \text{ \AA}$ and $c = 8.66 \text{ \AA}$, and $\text{Li}_2\text{Cr}_{0.5}\text{Mn}_{1.5}\text{O}_4$ has a diffraction pattern corresponding to a tetragonal cell of approximate dimensions $a = 5.70 \text{ \AA}$ and $c = 8.98 \text{ \AA}$. To compare the effect of chromium substitution on the crystallographic cell volume over the full range of compositions, a normalized

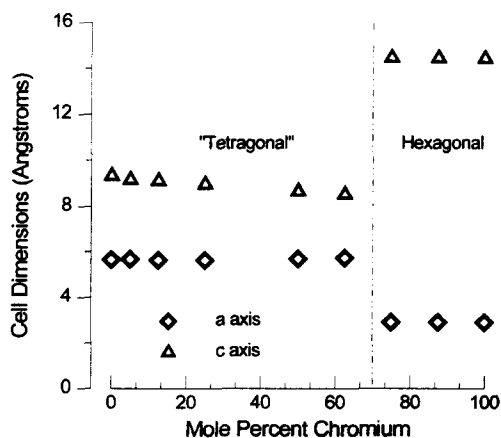


Fig. 1. Crystallographic cell dimensions of $\text{Li}_2\text{Cr}_x\text{Mn}_{2-x}\text{O}_4$ for $0 \leq x \leq 2$.

unit cell volume was defined. The normalized unit cell volume is taken as the crystallographic volume in \AA^3 , per stoichiometric unit comprising two lithium atoms, two transition metal atoms and four oxygen atoms. Fig. 2 shows the variation in normalized unit cell volume over the full range of compositions for $\text{Li}_2\text{Cr}_x\text{Mn}_{2-x}\text{O}_4$. The unit cell volume decreases smoothly with increasing chromium content as chromium(III), with a smaller ionic radius, is substituted for manganese(III). For phases within the hexagonal range of compositions an expansion in both the a - and c -axes occurs as the chromium content decreases. The tetragonal unit cell of $\lambda\text{-Li}_2\text{Mn}_2\text{O}_4$ is attributed to a cooperative Jahn–Teller distortion caused by the manganese(III) ion. In $\text{Li}_2\text{Cr}_x\text{Mn}_{2-x}\text{O}_4$ phases with the $\lambda\text{-Li}_2\text{Mn}_2\text{O}_4$ -type structure, the tetragonal distortion decreases in magnitude as chromium(III) is substituted for manganese(III). Thus, the contraction in volume with increasing chromium composition is asymmetric while the c -axis shrinking and the a -axis is expanding.

The X-ray diffraction patterns of $\text{Li}_2\text{Cr}_x\text{Mn}_{2-x}\text{O}_4$ phases for a range of compositions with the $\lambda\text{-Li}_2\text{Mn}_2\text{O}_4$ -type structure are shown in Fig. 3. Closer examination of the diffraction patterns reveals that these lattices have a small orthorhombic distortion, which is most easily seen in the expanded view of Fig. 4, by the splitting of the $\{400\}$ into (400) and (040) . Since the relative intensities of the reflections are very similar to those of $\lambda\text{-Li}_2\text{Mn}_2\text{O}_4$, the appropriate space group is possibly $Imma$ with the transition metals occupying the $4b$ and $4c$ sites, lithium atoms in the $4a$ and $4d$ positions, and oxygen in the $8i$ and $8h$ sites.

The potentials and shapes of charge/discharge cycles of cells built with $\text{Li}_2\text{Cr}_x\text{Mn}_{2-x}\text{O}_4$ cathodes vary with composition in a regular manner, as demonstrated in Fig. 5. Cells, not shown, with cathode compositions where $x \geq 1.75$, had significantly less reversible capacity, within the test conditions used, than those with more

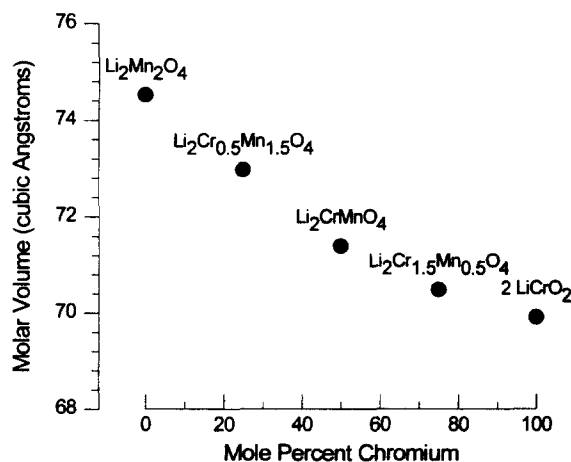


Fig. 2. Normalized crystallographic cell volumes per mole of $\text{Li}_2\text{Cr}_x\text{Mn}_{2-x}\text{O}_4$ as a function of composition for $0 \leq x \leq 2$.

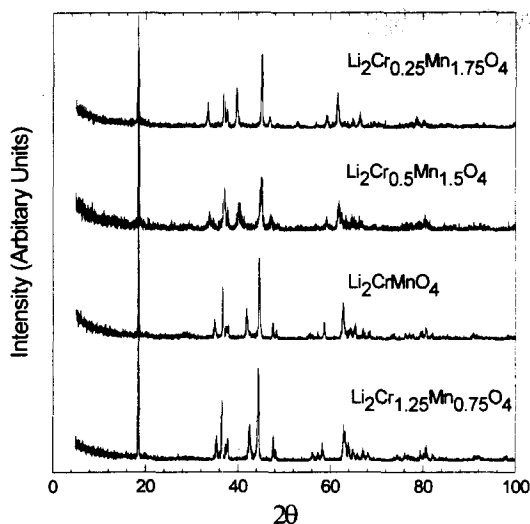


Fig. 3. X-ray powder diffraction patterns for $\text{Li}_2\text{Cr}_x\text{Mn}_{2-x}\text{O}_4$ phases with a $\lambda\text{-Li}_2\text{Mn}_2\text{O}_4$ -type structure.

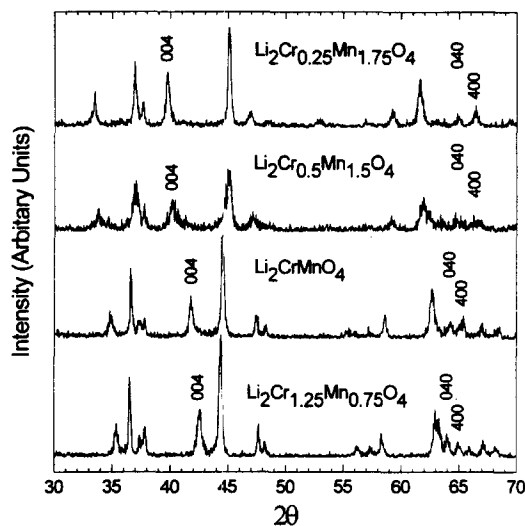


Fig. 4. Detailed view of $\text{Li}_2\text{Cr}_x\text{Mn}_{2-x}\text{O}_4$ diffraction patterns from 30 to 70° 2θ .

manganese-rich compositions. The electrochemical potential of $\lambda\text{-Li}_{2-y}\text{Mn}_2\text{O}_4$ has a distinct step at $y=1$, which is associated with a change of lithium occupancy from octahedral to tetrahedral sites. In $\lambda\text{-Li}_{2-y}\text{Mn}_2\text{O}_4$, this voltage step coincides with a crystallographic phase change from a tetragonal unit cell to a cubic one which results from a cooperative Jahn–Teller distortion that occurs at an average manganese valence of 3.5. This step also occurs in the tetragonal phases of $\text{Li}_2\text{Cr}_x\text{Mn}_{2-x}\text{O}_4$ with $x < 1$, but the depth-of-charge at which it occurs decreases with increasing chromium substitution. All compositions of $\text{Li}_2\text{Cr}_x\text{Mn}_{2-x}\text{O}_4$ have a higher average discharge potential and energy density than $\lambda\text{-Li}_2\text{Mn}_2\text{O}_4$.

Fig. 6 compares the accessible cathode capacity, in terms of percent lithium cycled, on the first charge and discharge of lithium-ion cells with petroleum coke an-

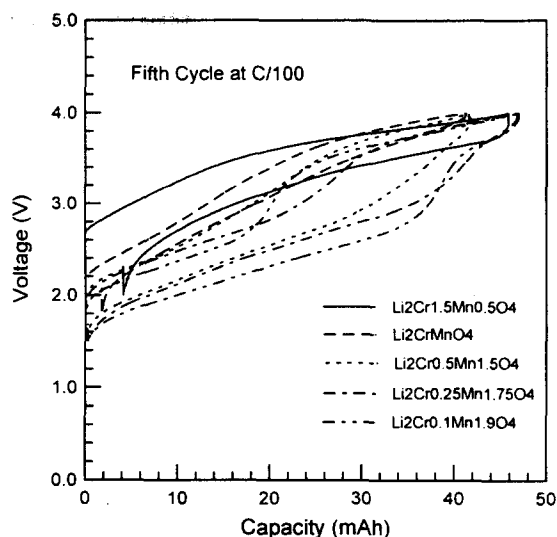


Fig. 5. The fifth charge/discharge cycle for coin cells with $\text{Li}_2\text{Cr}_x\text{Mn}_{2-x}\text{O}_4$ cathodes and carbon coke anodes.

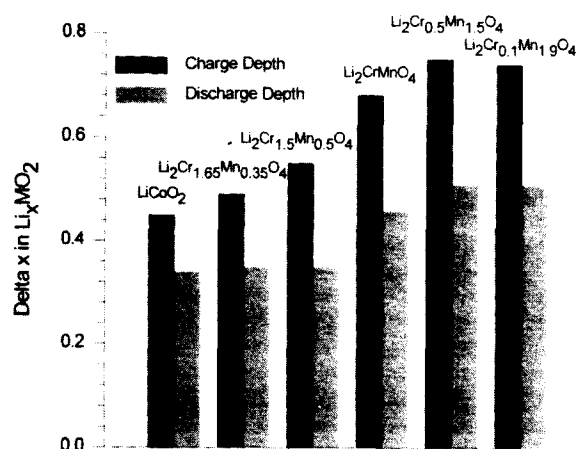


Fig. 6. Charge and discharge cathode utilization in lithium-ion cells cycled between 1.5 and 4.0 V at 100 h rate.

odes. The anode to cathode weight ratios were chosen to optimize the cathode capacity accessible below 4 V. These results are, however, each based on only one or two cells and may have a significant margin of variability. In all cases the reversible capacity, or discharge capacity, is at least as good as that of a similar LiCoO_2 cell. Compositions of $\text{Li}_2\text{Cr}_x\text{Mn}_{2-x}\text{O}_4$ with a spinel-related structure have greater capacity to 4.0 V than those with 3R-type hexagonal structure. This could be due to either differences in the intrinsic stability of the de-intercalated structure or to increases in cell potentials with increasing chromium content. The irreversible capacity losses, the differences between the charge depth and the discharge depth, are larger for all $\text{Li}_2\text{Cr}_x\text{Mn}_{2-x}\text{O}_4$ compositions than for cells with LiCoO_2 cathodes, but are comparable to that expected for a $\lambda\text{-Li}_2\text{Mn}_2\text{O}_4$ lithium-ion cell cycled to 4.0 V [6]. Figs. 7 and 8 demonstrate that lithium-ion cells with $\text{Li}_2\text{Cr}_x\text{Mn}_{2-x}\text{O}_4$ cathodes can be cycled to greater than

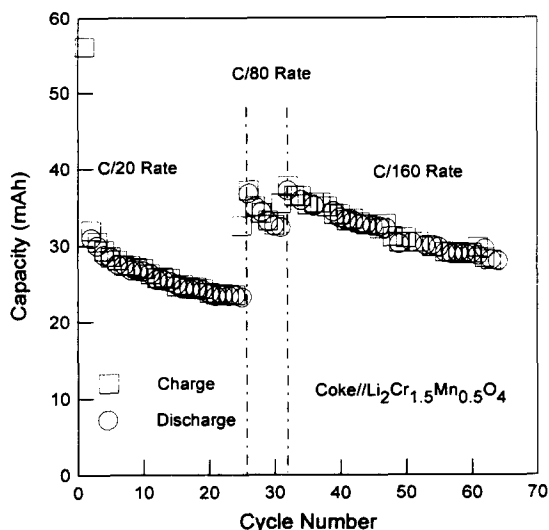


Fig. 7. Charge and discharge capacity as a function of cycle number for a lithium-ion cell with a $\text{Li}_2\text{Cr}_{1.5}\text{Mn}_{0.5}\text{O}_4$ cathode and a petroleum coke anode.

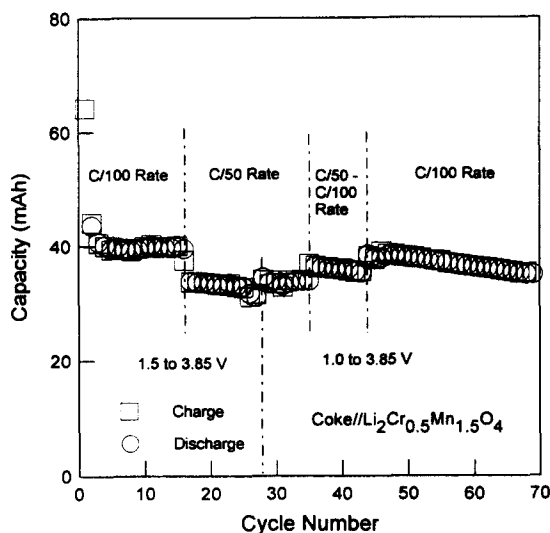


Fig. 8. Charge and discharge capacity as a function of cycle number for a lithium-ion cell with a $\text{Li}_2\text{Cr}_{0.5}\text{Mn}_{1.5}\text{O}_4$ cathode and a petroleum coke anode.

60 cycles at modest rates. The cycling rates were varied over the course of the experiment to examine the effect of rate on capacity and cycle life. The rate designation

$C/100$ means that it took 100 h to fully discharge, or charge, the cell. The cell containing a $\text{Li}_2\text{Cr}_{1.5}\text{Mn}_{0.5}\text{O}_4$ cathode, Fig. 7, was cycled between voltage limits of 1.8 and 4.0 V. The voltage limits of the $\text{Li}_2\text{Cr}_{0.5}\text{Mn}_{1.5}\text{O}_4$ cell, Fig. 8, were changed from 1.5 to 3.85 V to 1.0 to 3.85 V on the 28th cycle. The coin cell format, 2325, required that the electrodes have thickness of the order of 1 mm. Thinner electrodes will presumably have better rate capabilities.

4. Summary

Substituting a small amount of manganese (10% or perhaps less) for chromium in LiCrO_2 dramatically changes the material's color and electrochemical activity. Similarly, substituting even a small amount of chromium for manganese in $\lambda\text{-Li}_2\text{Mn}_2\text{O}_4$ stabilizes the structure. Unlike $\lambda\text{-Li}_2\text{Mn}_2\text{O}_4$, $\text{Li}_2\text{Cr}_x\text{Mn}_{2-x}\text{O}_4$ with $0 < x \leq 1.25$ can be prepared by direct solid-state reaction, and the products are air and thermally stable. $\text{Li}_2\text{Cr}_x\text{Mn}_{2-x}\text{O}_4$ phases have been shown to be practical materials for use as cathodes in lithium-ion cells.

Acknowledgements

The authors gratefully acknowledge the technical assistance of Martin Larabie, Gerald Pleizier, Gifford Shearer, Paul Helm and Roopa Ganapathy.

References

- [1] R. Hoppe, G. Brachtel and M. Jansen, *Z. Anorg. Allg. Chem.*, **417** (1975) 1–10.
- [2] A. Mosbah, A. Verbaere and M. Tournoux, *Mater. Res. Bull.*, **18** (1983) 1375–1381.
- [3] G. Pistoia, G. Wang and C. Wang, *Solid State Ionics*, **58** (1992) 285–292.
- [4] B. Wang, Y. Xia, L. Feng and D. Zhao, *J. Power Sources*, **43/44** (1993) 539–546.
- [5] W.I.F. David, M.M. Thackeray, L.A. De Picciotto and J.B. Goodenough, *J. Solid State Chem.*, **67** (1987) 316–323.
- [6] J.M. Tarascon and D. Guyomard, *J. Electrochem. Soc.*, **138** (1991) 2864–2868.